멤브레인(Membrane Journal)
Vol. 28 No. 2 April, 2018, 121-128

Print ISSN: 1226-0088
Online ISSN: 2288-7253
DOI: https://doi.org/10.14579/MEMBRANE_JOURNAL.2018.28.2.121

PBEM-PMMA-POEM 터폴리머 분리막의 합성, 분석 및 기체 분리 성능

박 병 주·김 나 운·박 정 태*·김 종 학†

연세대학교 화공생명공학과, *건국대학교 화학공학과
(2018년 4월 24일 접수, 2018년 4월 29일 수정, 2018년 4월 29일 채택)

Synthesis, Characterizations and Gas Separation Property of PBEM-PMMA-POEM Terpolymer Membranes

Byeong Ju Park, Na Un Kim, Jung Tae Park*, and Jong Hak Kim†

Department of Chemical and Biomolecular Engineering, Yonsei University, 50 Yonsei-ro, Seodaemun-gu, Seoul 03722, South Korea

*Department of Chemical Engineering, Konkuk University, 120 Neungdong-ro, Gwangjin-gu, Seoul 05029, South Korea
(Received April 24, 2018, Revised April 29, 2018, Accepted April 29, 2018)

요 약: 세 가지의 다른 화학 성분으로 구성된 터폴리머는 기체분리막에 거의 활용되지 못하였다. 본 연구에서는 poly(2-[3-(2H-Benzotriazol-2-yl)-4-hydroxyphenyl] ethylmethacrylate)(PBEM), poly(oxyethylene methacrylate)(POEM), methyl methacrylate (MMA)로 구성된 터폴리머를 자유라디칼 중합법으로 합성하였고, 이를 기반으로 하여 이산화탄소/질소 분리를 위한 복합막 제조 공정을 개발하였다. 합성된 PBEM-PMMA-POEM 용액을 다공성 폴리설폰 지지체위에 코팅하여 복합막을 제조하였다. 성공적인 중합, 특성 및 구조분석을 위하여 푸리에 변환 적외선 분광학, X-ray 회절분석법, 열중량 분석 및 전계 방사 주사전자 현미경을 사용하였다. PBEM-PMMA-POEM 터폴리머 분리막의 기체 투과도 및 이산화탄소/질소 선택도를 25°C에서 측정하였다. 최고의 이산화탄소/질소 선택도는 30.2에 도달하였으며, 이산화탄소 투과도는 57.4 GPU (1 GPU = 10^{-6} cm^3(STP)/(s cm^2 cmHg))이었다.

Abstract: Terpolymers, which are chemical compounds composed of three different chemical compounds, have rarely been utilized for gas separation membranes. In this study, we demonstrate a simple process to fabricate a composite membrane for CO_2/N_2 separation based on a terpolymer synthesized from poly(2-[3-(2H-benzotriazol-2-yl)-4-hydroxyphenyl] ethylmethacrylate)(PBEM), poly(oxyethylene methacrylate)(POEM), and methyl methacrylate (MMA) via free radical polymerization. A solution of the as-synthesized PBEM-PMMA-POEM was coated onto a microporous polysulfone (PSf) support to form a composite membrane. The successful polymerization and the characteristics and morphology of the membrane were characterized by Fourier transform infrared spectroscopy (FT-IR), X-ray diffraction (XRD) analysis, thermogravimetric analysis (TGA), and field emission scanning electron microscopy (FE-SEM). The gas permeance and CO_2/N_2 selectivity of the PBEM-PMMA-POEM terpolymer membrane were measured at 25°C. A maximum CO_2/N_2 selectivity of 30.2 was obtained at a CO_2 permeance of 57.4 GPU (1 GPU = 10^{-6} cm^3(STP)/(s cm^2 cmHg)).

***Keywords**: composite membrane, terpolymer, gas separation, selectivity, free radical polymerization*

1. Introduction

Gas separation processes based on polymeric membranes have attracted great attention due to their many technical advantages, such as high energy efficiency, easy scale-up, simple processing, and low operating costs[1-4]. Furthermore, membrane gas separation units are safe and environmentally friendly due to the absence of mechanical complexity. In particular, there

†Corresponding author(e-mail: jonghak@yonsei.ac.kr, http://orcid.org/0000-0002-5858-1747)

have been significant developments in CO_2/N_2, CH_4/N_2, and CO_2/H_2 separation using polymeric membranes to reduce the emission of greenhouse gases[5-7]. During the last few years, composite membranes consisting of two different matrices have been developed in order to improve the performance of separation membranes [8-10]. Such membranes can combine the advantages of both materials in a single membrane.

Amphiphilic copolymers are comprised of separate hydrophilic and hydrophobic segments, enabling the chains to self-assemble at the nanometer scale[11-12]. In general, the hydrophobic segments provide good mechanical strength while the hydrophilic segments provide the functionality of the membrane. One class of amphiphilic copolymers is amphiphilic block copolymers, in which the homopolymers are clearly divided into two parts. These copolymers show a highly ordered structure and good performance. However, the synthesis of block copolymers is usually carried out via anionic polymerization, which is sensitive to impurities and the environment[13-14]. The synthesis of graft copolymers, which consist of a linear backbone of one chain and randomly connected branches of the other chain, is easier and less sensitive compared to that of block copolymers. Graft copolymers with highly ordered nanostructures have been produced via control of the polymer-solvent interaction[15-16]. Terpolymers, which are chemical compounds composed of three different chemical compounds, have rarely been utilized for gas separation membranes.

Mass transport through the polymeric membrane during gas separation is described by the solution-diffusion mechanism[17]. According to this model, permeability is the product of the solubility coefficient (thermodynamic factor) and the diffusion coefficient (kinetic parameter). The permeance of CO_2 is intrinsically higher than that of N_2 due to its high solubility (high condensation temperature) and high diffusivity (small kinetic diameter), and thus it is feasible to prepare commercially attractive polymer membranes for CO_2/N_2 separation.

Polymers based on poly (ethylene oxide)(PEO) were chosen as a candidate for CO_2 separation due to its CO_2-philicity and CO_2 separation properties[18-19]. The drawback of PEO in such membranes is its tendency to crystallize, which reduces the permeable amorphous soft volume fractions and chain mobility, leading to a decrease in gas permeability and selectivity. Lee et al. reported a comb copolymer synthesized using poly(oxyethylene methacrylate)(POEM) and poly(2-[3-(2H-benzotriazol-2-yl)-4-hydroxyphenyl] ethylmethacrylate)(PBEM). POEM is a PEO analogue with high CO_2 affinity, and has the advantage of an amorphous structure. This polymer was once considered to be of limited for use in membranes because of its liquid-like nature. However, this is compensated by the rigid, hydrophobic BEM segments in this polymer membrane[20].

In this work, we demonstrate a simple process to fabricate a composite membrane for CO_2/N_2 separation based on a terpolymer synthesized from PBEM, POEM, and methyl methacrylate (MMA) via free radical polymerization. A solution containing the as-synthesized PBEM-PMMA-POEM was coated onto a polysulfone (PSf) substrate. The PBEM-PMMA-POEM terpolymer was developed in order to increase CO_2 permeance due to its high CO_2 affinity. The structural, thermal, and morphological properties of the membrane were characterized using Fourier transform infrared spectroscopy (FT-IR), X-ray diffraction (XRD) analysis, thermogravimetric analysis (TGA), and field emission scanning electron microscopy (FE-SEM). The pure gas permeance and CO_2/N_2 selectivity of the PBEM-PMMA-POEM terpolymer membrane were measured at 25°C.

2. Experimental Section

2.1. Materials

2-[3-(2H-Benzotriazol-2-yl)-4-hydroxyphenyl] ethylmethacrylate (BEM, M_w = 323 g/mol), poly (oxyethylene methacrylate) (POEM), poly (ethyleneglycol)methylethermethacrylate, M_n = 500 g/mol), methyl methacrylate (MMA, 99%), azobisisobutyronitrile (AIBN), and poly[1-(trimethylsilyl)-1-propyne] (PTMSP) were

purchased from Sigma Aldrich. N-hexane, cyclohexane, N,N-dimethylformamide (DMF), isopropyl alcohol (IPA), acetonitrile, methanol (MeOH, 99.9%), ethanol (EtOH, 99.9%), and dimethyl sulfoxide (DMSO, 99.9%) were obtained from J. T. Baker. The polysulfone (PSf) substrate was provided by Toray Chemical Korea Inc. All solvents and chemicals were of reagent grade and were used as received without any treatment.

2.2. Synthesis of the terpolymer PBEM-PMMA-POEM

For the synthesis of the terpolymer, a weight ratio of 1 : 1 : 8 (PBEM : MMA : POEM) was used. First, 1 g of the BEM monomer was completely dissolved in 70 mL of DMF under stirring for 1 h, and then 1 mL MMA and 8 mL POEM were added to the solution. Subsequently, 0.002 g of AIBN was added to the solution to initiate the free-radical polymerization. After purging the mixed solution with nitrogen gas for an hour, it was placed in a 90°C oil bath for 20 h to allow the free radical polymerization to occur. The viscosity of the solution increased during this time. The resultant solution was precipitated in an n-hexane:IPA (8:2) mixture. To eliminate impurities and residual monomers, this dissolution-precipitation process was repeated three times, and the resulting polymer was dried completely in a vacuum oven. The final weight of polymer obtained was 4.22 g.

2.3. Preparation of the PBEM-PMMA-POEM composite membrane

First, a 0.5% solution of PTMSP in cyclohexane was coated onto the microporous PSf support (average pore size = 0.5 μm, Toray Chemical Inc.) as a gutter layer using an RK-coater (Model 101, Control RK Print-Coat Instruments Ltd., UK) to minimize the effect of the porous structure of the support and the penetration of the coating solution. Then, a 20% solution of PBEM-PMMA-POEM in EtOH was coated onto the PTMSP-coated PSF support using the RK-coater. After the coating process, the membrane was dried in a vacuum oven overnight to remove the solvent completely.

2.4. Characterizations

FT-IR spectra of the synthesized copolymer were obtained in the frequency range from 4000 to 500 cm^{-1} with an Excalibur series FT-IR instrument (DIGLAB CO., Hannover, Germany) to confirm the successful polymerization. XRD patterns of the sample were collected at 30 kV and 15 mA for structural analysis. The morphologies of the fabricated membranes were characterized using a field emission scanning electron microscope (FE-SEM, JSM-7001F, JEOL Ltd., Japan). The thermal stability of the terpolymer was investigated by TGA (TGA/DSC1, Mettler Toledo, Korea) at heating rate of 20°C min^{-1} in an air atmosphere.

2.5. Gas permeation measurements

Gas permeance tests were conducted at 25°C with the constant pressure/variable volume method using gas separation equipment from Airrane Co. Ltd (Korea). The permeance was measured in gas permeation units (GPU); 1 GPU equal 10^{-6} $cm^3(STP)/s \cdot cm^2 \cdot cmHg$. The selectivity of the membrane was calculated by the ratio of the permeances of the gases, in this case, the permeability of the more permeable gas, CO_2, was divided by that of the less permeable gas, N_2. The gas permeance of the membrane was measured for 2 h using the individual gases to determine their steady-state performance, and the flowrate measurements were taken under pressures of 1 to 5 bar to investigate the effect of changes in pressure on the permeability and selectivity of the membrane.

3. Results and Discussion

3.1. Synthesis and properties of the terpolymer PBEM-PMMA-POEM terpolymer

The terpolymer PBEM-PMMA-POEM was synthesized via a facile one-step free radical polymerization using AIBN as an initiator at 90°C, as shown in Fig. 1. The PBEM-PMMA-POEM terpolymer was designed to exhibit a microphase-separated structure composed of hydrophobic PBEM and PMMA domains and hydrophilic POEM domains. The hydrophobic PBEM and

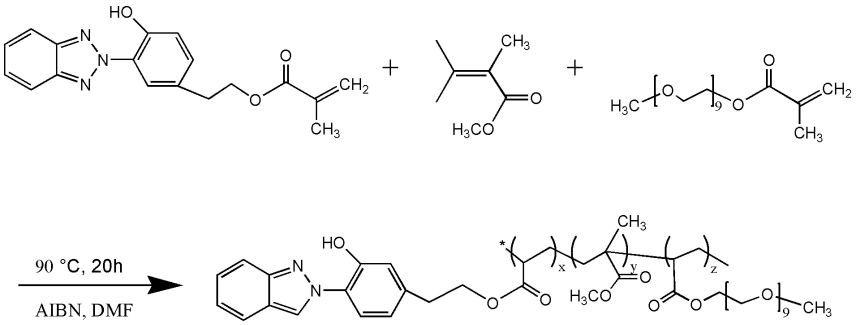

Fig. 1. Synthesis of the PBEM-PMMA-POEM terpolymer via radical polymerization using the initiator AIBN.

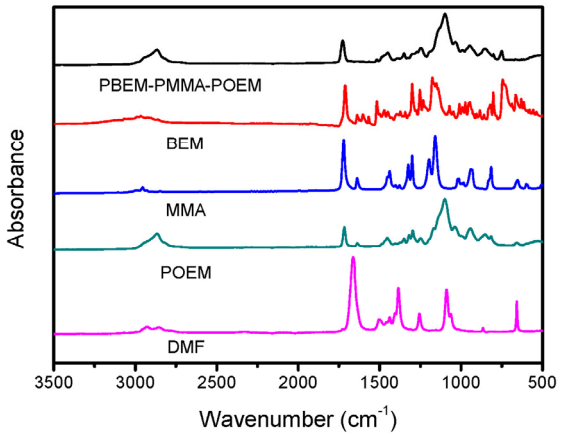

Fig. 2. FT-IR spectra of the PBEM-PMMA-POEM terpolymer, BEM, MMA, POEM, and the solvent DMF.

PMMA domains contributed rigid properties to the terpolymer, while the hydrophilic POEM domains imbued rubbery characteristics. Moreover, the three tertiary amines in the triazole units of the PBEM chains have a high CO_2 uptake, which compensates for the poor mechanical properties of the POEM chains. As a result, the fabricated membrane was expected to exhibit high CO_2 permeance and plasticization resistance without a drastic decrease in CO_2 permeance at high pressure.

As shown in Fig. 2, the FT-IR spectrum confirmed the successful synthesis of the PBEM-PMMA- POEM terpolymer. FT-IR spectra of the three monomers (BEM, MMA, POEM) and of the solvent DMF were also recorded. The absorption bands at 1715 cm^{-1} for BEM and 1717 cm^{-1} in the POEM spectrum were assigned to the stretching vibrations of the C=O double bond. This vibrational peak shifted to a higher wavenumber of 1728 cm^{-1} in PBEM-PMMA-POEM, which indicated an increase in the strength of the C=O double bond. The BEM, MMA, and POEM monomers all exhibited a weak band at 1637 cm^{-1}, which originated from the C=C stretching vibration of the methacrylate moiety. This band was not observed in the spectrum of the PBEM-PMMA-POEM terpolymer after polymerization, which indicated that the free radical polymerization was completed and that no residual monomer was present in the resulting terpolymer. The PBEM-PMMA-POEM terpolymer showed a significant broad peak at 2865 cm^{-1}, which originated from the O-H stretching vibrations of the POEM domains. The absorption band at 1516 cm^{-1} in the spectrum of the monomer BEM was associated with the stretching vibrational mode of the aromatic ring, and was significantly decreased in the spectrum of the PBEM-PMMA-POEM copolymer. The strong absorption band of the PBEM-PMMA-POEM copolymer at 1100 cm^{-1} was due to the stretching vibration mode of the ether (C-O-C) groups resulting from the POEM domains. Finally, the absorption band at 750 cm^{-1} in the PBEM-PMMA-POEM terpolymer spectrum was assigned to the bending mode of the aromatic C-H ring, and appeared at slightly higher wavenumber compared to the BEM aromatic C- H ring. No DMF solvent peaks were observed in the spectrum of the PBEM-PMMA-POEM terpolymer, suggesting that DMF was completely removed.

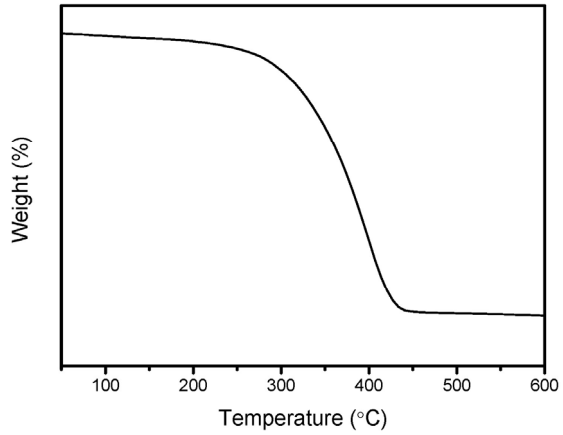

Fig. 3. TGA curve of the PBEM-PMMA-POEM terpolymer.

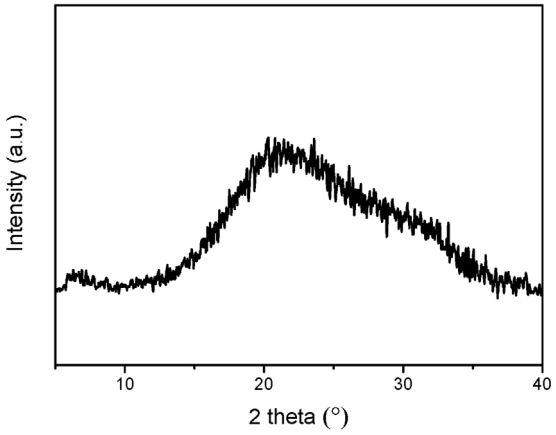

Fig. 4. XRD pattern of the PBEM-PMMA-POEM terpolymer.

3.2. Structural, thermal, and morphological properties

The results of the TGA analysis are shown in Fig. 3. As shown in the TGA curve, the PBEM-PMMA-POEM terpolymer demonstrated thermal stability up to 250°C; degradation was observed upon heating above this temperature. This result indicated that the terpolymer had good thermal stability. The TGA curves of POEM and PBEM measured by Lee et al. showed thermal degradation at approximately 150°C, and those of other POEM-POEM copolymers showed degradation at approximately 250°C, which did not differ significantly from the PBEM-PMMA-POEM copolymer [20]. The improved thermal stabilities of the polymers compared to the individual components may have resulted from the increased molecular weight and intermolecular forces after polymerization.

Fig. 4 shows the XRD patterns of the PBEM-PMMA-POEM terpolymer. The absence of a sharp crystalline peak demonstrates that this terpolymer has an amorphous structure. A broad main peak was observed at 2θ = 20. 5°, and a shoulder peak was observed at 2θ = 32°. This XRD pattern was compared to those reported for other similar polymers in the literature. The POEM and PBEM homopolymer patterns reported by Lee et al. showed peaks at 2θ = 20.2° and 11.7°, respectively. Islam et al. reported that the broad peak of the PMMA homopolymer was located at 2θ = 30°, which is in good agreement with our results[20,21]. The d-spacing values calculated using Bragg's law for these peaks were 4.4 Å and 3.0 Å. For PBEM-PMMA-POEM terpolymer, the peak at 2θ = 20.5° is believed to correspond to correspond to the peak of POEM at 20.2°, and the peak at 32° was thought to be related to the PMMA peak at 30°. These XRD results suggest that overall, the copolymerization was successful based on the evidence of POEM and PMMA nanostructures in the terpolymer; the PBEM peak was not significantly expressed because of the low ratio of PBEM used in the synthesis.

3.3. Gas separation performance of the PBEM-PMMA-POEM/PSf composite membrane

The PBEM-PMMA-POEM terpolymer composite membrane was prepared by coating a 20 wt% solution of the terpolymer onto the PTMSP-coated PSF supporting layer using an RK control coater. The PTMSP gutter layer was used to ensure good coating of the terpolymer, and prevented intrusion of the coating solution into the porous PSf supporting layer. While this gutter layer did not affect the gas separation performance of the membrane due to its thinness, it helped to prevent undesirable defects in the coating layer.

The cross-sectional and surface morphologies of the PBEM-PMMA-POEM/PSf composite membrane were observed using SEM, as shown in Fig. 5. A thin se-

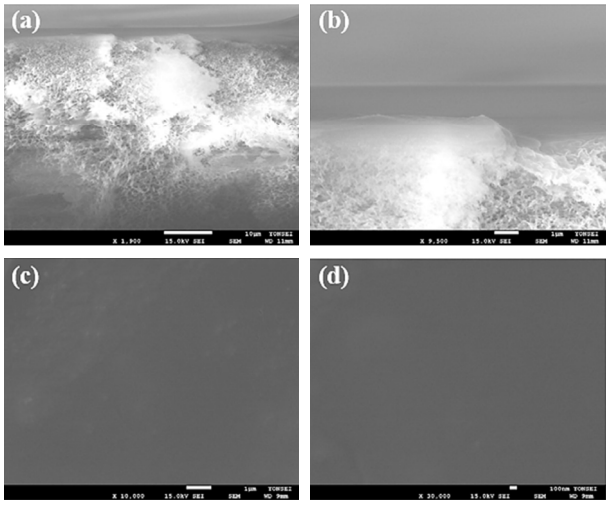

Fig. 5. SEM images of the PBEM-PMMA-POEM terpolymer membrane on a microporous PSf support: (a, b) cross-sectional images, and (c, d) surface images.

lective layer of the PBEM-PMMA-POEM terpolymer with a thickness of 1.845 μm was coated onto the PSMSP-coated PSf supporting layer. The intimate contact between the terpolymer coating layer and the PTMSP-coated PSf supporting layer was expected to ensure the durability and long-term stability of the composite membrane during operation. Fig. 4(c) and 4(d) show the uniformity of the surface, on which no defects or voids are observed.

The gas separation performance of the PBEM-PMMA-POEM membrane was first evaluated using single gas permeation tests at 25°C with feed pressures from 1 to 5 bar. The pure gas permeances and the ideal CO_2/N_2 selectivity of the PBEM-PMMA-POEM membrane with increasing feed pressure are shown in Fig. 6 and 7, respectively. As seen in Fig. 6, the pure CO_2 permeance was always higher than the pure N_2 permeance, regardless of the feed pressure. This was due to the higher diffusivity and the higher solubility of CO_2 as a result of its smaller kinetic diameter (3.30 Å) and higher condensability (195 K) compared to N_2 (3.64 Å and 71 K)[22,23]. The PBEM-PMMA-POEM terpolymer contains a polar group (the ether oxygen) in the flexible hydrophilic POEM chains that has high affinity for CO_2 molecules via dipole-quadrupole interactions.

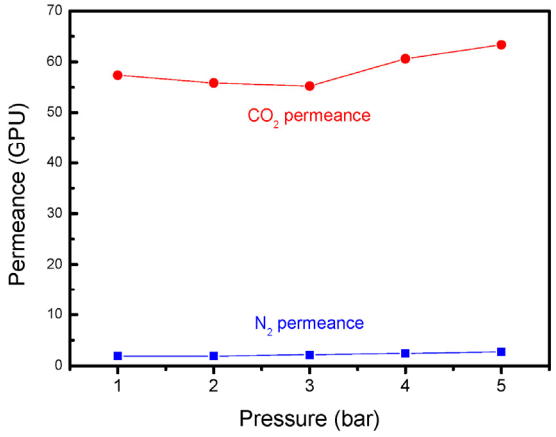

Fig. 6. CO_2 and N_2 gas permeances through the PBEM-PMMA-POEM membrane at 25°C and different feed pressures.

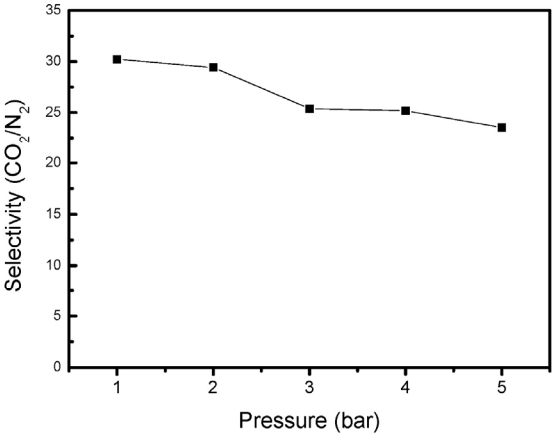

Fig. 7. Ideal selectivity of CO_2/N_2 through the PBEM-PMMA-POEM membrane at 25°C and different feed pressures.

To investigate the plasticization phenomena, which could influence the gas separation performance of the membrane, the feed pressure was increased up to 5 bar. As the pressure increased, the permeance of both CO_2 and N_2 increased, except in the case of CO_2 at 1-3 bar. Increased pressure caused plasticization of the membranes, in which the polymer chains swell and the free volume of the membrane is increased. This swelling led to an increase in N_2 permeance, resulting in decreased CO_2/N_2 selectivity, as shown in Fig. 7 and Table 1. As a result, the CO_2/N_2 selectivity decreased from 30.2 to 23.6 as the pressure increased from 1 to 5 bar.

Table 1. Pure Gas Permeance and Ideal Selectivity of CO_2/N_2 through the PBEM-PMMA-POEM Membrane at Different Feed Pressures

Feed pressure	CO_2 permeance (GPU)	N_2 permeance (GPU)	Ideal selectivity (CO_2/N_2)
1 bar	57.4	1.9	30.2
2 bar	55.9	1.9	29.4
3 bar	55.2	2.2	25.4
4 bar	60.6	2.4	25.2
5 bar	63.4	2.7	23.6

4. Conclusions

In conclusion, we fabricated a high-performance gas separation membrane based on the CO_2-philic terpolymer PBEM-PMMA-POEM, which was synthesized via free radical polymerization. The PBEM-PMMA-POEM terpolymer was composed of rigid hydrophobic BEM and MMA segments and flexible hydrophilic POEM segments. FT-IR spectroscopy and XRD analysis confirmed the successful synthesis of the targeted polymer and its amorphous structure. The thermal stability of the terpolymer at temperatures up to approximately 250°C was verified via TGA. The surface and cross-sectional morphologies of the PBEM-PMMA-POEM/PSf composite membrane were observed using SEM. Gas permeation tests of the membrane showed its high selectivity for CO_2 over N_2. The presence of polar groups (ether oxygens) that have high affinity for CO_2 molecules via dipole-quadrupole interactions in the flexible hydrophilic POEM chains enhanced the CO_2 permeance. The CO_2/N_2 selectivity of the PBEM-PMMA-POEM membrane reached 30.2 at a CO_2 permeance of 57.4 GPU. An additional advantage of the PBEM-PMMA-POEM terpolymer reported here is the low cost of its synthesis due to the utilization of free radical polymerization rather than the anionic polymerization techniques that are typically used for conventional block copolymers.

Acknowledgements

This work was supported by a National Research Foundation (NRF) grant funded by the Ministry of Science, ICT and Future Planning (NRF-2017R1A4 A1014569, NRF-2017R1D1A1B06028030).

Reference

1. S. Luo, Q. Liu, B. Zhang, J. R. Wiegand, B. D. Freeman, and R. Guo, "Pentiptycene-based polyimides with hierarchically controlled molecular cavity architecture for efficient membrane gas separation", *J. Membr. Sci.*, **480**, 20 (2015).
2. Y. Zhuang, J. G. Seong, Y. S. Do, H. J. Jo, Z. Cui, J. Lee, Y. M. Lee, and M. D. Guiver, "Intrinsically microporous soluble polyimides incorporating Tröger's base for membrane gas separation", *Macromolecules*, **47**, 3254 (2014).
3. R. W. Baker and B. T. Low, "Gas separation membrane materials: A perspective", *Macromolecules*, **47**, 6999 (2014).
4. Y. Peng, Y. Li, Y. Ban, and W. Yang, "Two-dimensional metal-organic framework nanosheets for membrane-based gas separation", *Angew. Chem. Int. Ed.*, **56**, 9757 (2017).
5. L. Xiang, Y. Pan, G. Zeng, J. Jiang, J. Chen, and C. Wang, "Preparation of poly(ether-block-amide)/attapulgite mixed matrix membranes for CO_2/N_2 separation", *J. Membr. Sci.*, **500**, 66 (2016).
6. C. Sun, B. Wen, and B. Bai, "Application of nanoporous graphene membranes in natural gas process-

ing: Molecular simulations of CH_4/CO_2, CH_4/H_2S and CH_4/N_2 separation", *Chem. Eng. Sci.*, **138**, 616 (2015).
7. C. H. Park, J. H. Lee, M. S. Park, and J. H. Kim, "Facilitated transport: basic concepts and applications to gas separation membranes", *Membr. J.*, **27**, 205 (2017).
8. K. W. Ki and S. W. Kang, "1-Butyl-3-methylimidazolium tetrafluoroborate/Al_2O_3 composite membrane for CO_2 separation", *Membr. J.*, **27**, 226 (2017).
9. L. Zhao, Y. Chen, B. Wang, C. Sun, S. Chakraborty, K. Ramasubramanian, P. K. Dutta, and W. S. W. Ho, "Multilayer polymer/zeolite Y composite membrane structure for CO_2 capture from flue gas", *J. Membr. Sci.*, **498**, 1 (2016).
10. Y. Zhang, X. Feng, S. Yuan, J. Zhou, and B. Wang, "Challenges and recent advances in MOF-polymer composite membranes for gas separation", *Inorg. Chem. Front.*, **3**, 896 (2016).
11. W. Ma, S. Rajabzadeh, A. R. Shaikh, Y. Kakihana, Y. Sun, and H. Matsuyama, "Effect of type of poly(ethylene glycol)(PEG) based amphiphilic copolymer on antifouling properties of copolymer/poly(vinylidene fluoride)(PVDF) blend membranes", *J. Membr. Sci.*, **514**, 429 (2016).
12. W. Wang, J. Lin, C. Cai, and S. Lin, "Optical properties of amphiphilic copolymer-based self-assemblies", *Eur. Polym. J.*, **65**, 112 (2015).
13. M. J. Derry, L. A. Fielding, and S. P. Armes, "Polymerization-induced self-assembly of block copolymer nanoparticles via RAFT non-aqueous dispersion polymerization", *Prog. Polym. Sci.*, **52**, 1 (2016).
14. B. Sarkar and P. Alexandridis, "Block copolymer-nanoparticle composites: Structure, functional properties, and processing", *Prog. Polym. Sci.*, **40**, 33 (2015).
15. W. S. Chi, S. J. Kim, S. J. Lee, Y. S. Bae, and J. H. Kim, "Enhanced performance of mixed-matrix membranes through a graft copolymer-directed interface and interaction tuning approach", *Chem. Sus. Chem.*, **8**, 650 (2015).
16. J. Y. Lim, C. S. Lee, J. M. Lee, J. M. Ahn, H. H. Cho, and J. H. Kim, "Amphiphilic block-graft copolymer templates for organized mesoporous TiO_2 films in dye-sensitized solar cells, *J. Power Sources*, **301**, 18 (2016).
17. P. Sun, K. Wang, and H. Zhu, "Recent developments in graphene-based membranes: Structure, mass-transport mechanism and potential applications", *Adv. Mater.*, **28**, 2287 (2016).
18. S. Quan, Y. P. Tang, Z. X. Wang, Z. X. Jiang, R. G. Wang, Y. Y. Liu, and L. Shao, "PEG-imbedded PEO membrane developed by a novel highly efficient strategy toward superior gas transport performance", *Macromol. Rapid Commun.*, **36**, 490 (2015).
19. C. Zhang, P. Li, and B. Cao, "Effects of the side groups of the spirobichroman-based diamines on the chain packing and gas separation properties of the polyimides", *J. Membr. Sci.*, **530**, 176 (2017).
20. J. H. Lee, J. P. Jung, E. Jang, K. B. Lee, Y. S. Kang, and J. H. Kim. "CO_2-philic PBEM-g-POEM comb copolymer membranes: Synthesis, characterization and CO_2/N_2 separation", *J. Membr. Sci.*, **502**, 191 (2016).
21. M. S. Islam, J. H. Yeum, and A. K. Das, "Synthesis of poly(vinyl acetate-methyl methacrylate) copolymer microspheres using suspension polymerization", *J. Colloid Interface Sci.*, **368**, 400 (2012).
22. A. Brunetti, F. Scura, G. Barbieri, and E. Drioli, "Membrane technologies for CO_2 separation", *J. Membr. Sci.*, **359**, 115 (2010).
23. P. Bernardo, E. Drioli, and G. Golemme, "Membrane gas separation: A review/state of the art", *Ind. Eng. Chem. Res.*, **48**, 4638 (2009).